Chiang Mai J. Sci. 2020; 47(1) : 98-113
http://epg.science.cmu.ac.th/ejournal/
Contributed Paper

Molecular Docking Study of Chromone Derivatives as Dual Inhibitor Against Plasmepsin II and Falcipain-2

Chirattikan Maicheen [a] and Jiraporn Ungwitayatorn*[b]

[a] Faculty of Pharmacy, Huachiew Chalermprakiet University, 18/18 Bang Na-Trad Road, Samut Prakarn 10540, Thailand.

[b] Faculty of Pharmacy, Mahidol University, 447 Sri-Ayudhya Road, Bangkok 10400, Thailand.

*Author for correspondence; e-mail: jiraporn.ung@mahidol.ac.th

Received: 25 April 2019
Revised: 17 July 2019
Accepted: 23 July 2019

Abstract

Malaria remains a major problem to human health and necessitates the need to continue the search for new effective drugs. In this study, a series of chromone compounds with potent antimalarial activity have been subjected to docking simulation study in order to preliminary evaluate the potential as dual inhibitor against plasmepsin II (PM II) and falcipain-2 (FP-2). The results revealed that compound **45** exhibited the best binding affinity (binding energy = -9.03 kcal/mol) to PM II and showed high binding affinity to FP-2 (binding energy = -7.43 kcal/mol). Compound **47** showed the strongest binding affinity (binding energy = -8.00 kcal/mol) against FP-2 and high binding with PM II (binding energy = -6.73 kcal/mol). Both compounds showed more tightly binding than the known dual PM II and FP-2 inhibitors, i.e., fisetin (binding energy = -6.53 and -4.97 kcal/mol against PM II and FP-2, respectively) and myricetin (binding energy = -5.51 and -4.78 kcal/mol against PM II and FP-2, respectively). Thus, chromone series have the potential to be a new class of antimalarial drug with dual PM II and FP-2 inhibitory activity.

Keywords: molecular docking, chromone derivatives, plasmepsin II, falcipain-2, dual inhibitor.

1. Introduction

Malaria has become more difficult to treat because of an increase in multi-drug resistant strains and unavailability of a successful vaccine [1]. Despite a long time efforts to eradicate or control the disease, it remains a major threat to public health of countries in tropical regions of the world [2]. This situation demands the discovery of new molecular targets within the parasite for the development of next generation antimalarial drugs. The aspartic protease plasmepsin II (PM II) and cysteine protease falcipain-2 (FP-2) are important antimalarial drug targets, especially combined inhibition of these two enzymes.

PM II is one of the four catalytically active plasmepsins (PM I, PM II, PM IV and histoaspartyl protease) that has been identified in the food vacuole of *Plasmodium falciparum* [3,4]. PM II is a 37 kDA enzyme with 329 amino acids. The active binding site of PM II contains eight subsites (S1-S4 and S1´-S4´). The key amino acid residues in the active site are the catalytic dyad Asp34 and Asp214, the flap residues Val78 (S2) and Ser79

(S1), and the residues Ser218 (S4) and Gly36 which are in proximity to the catalytic dyad. Most of the potent inhibitors form hydrogen bonds with these residues [5]. PM II is a key enzyme in the degradation of host hemoglobin which occurs inside acidic vacuoles of the parasite. The inhibition of the hemoglobin degradation pathway is lethal for the parasite [6].

FP-2 is a single polypeptide chain of 241 amino acids consisting of two distinct domains. These two domains are separated by a long central substrate binding cleft containing the active site [7,8]. The conserved catalytic residues of FP-2 are composed of Gln36, Cys42, His174 and Asn204 [9]. The active binding site contains three subsites (S1-S3). The hydrophobic S2 pocket is the major determinant of specificity for most cysteine proteases [10]. A series of possible hydrophobic interactions are found between the amino acids in enzyme active site and inhibitor, involving the nonpolar regions of Gln36, Asn173 (S1); Ser149, Ala175 (S2); Gly83, Tyr78, Leu84 (S3) [9]. FP-2 degrades hemoglobin at the early trophozoite stage and also responsible for the proteolytic activation of pro-PMs [7]. FP-2 inhibitor will block hemoglobin hydrolysis in the parasite food vacuole, thereby inhibiting parasite development.

PM II inhibitors are classified into peptidomimetics and non-peptidomimetics. Pepstatin A is a well-known peptidomimetic PM II inhibitor with IC_{50} value (50% inhibition of parasite growth against *P. falciparum*) = 4.00 μM [11] and inhibition constant (Ki) = 0.006 nM [12]. The main classes of falcipain-2 inhibitors are peptidomimetic inhibitors [13-14]. The peptidomimetic FP-2 inhibitors have ability to inhibit the enzyme at very low nanomolar range. However, peptidomimetic enzyme inhibitors normally exhibit low availability due to their high molecular weight, poor solubility, susceptible to proteolytic degradation. Another disadvantage of peptidomimetics is synthesis difficulties. Therefore, the non-peptidomimetic inhibitors are more interesting for developing the new PM II and FP-2 inhibitors.

Flavonoids, the natural phenyl substituted chromones, have been reported to exhibit the antimalarial activity against *P. falciparum* [15-17]. Kaempferol, myricetin, quercetin and luteolin can inhibit the intraerythrocytic growth of the chloroquine-sensitive (3D7) and chloroquine-resistant (7G8) strains of *P. falciparum*. The most active compound against both strains is luteolin with IC_{50} values of 11±1 μM and 12±1 μM for 3D7 and 7G8, respectively [16]. Several flavonoids, i.e., genistein, luteolin, kaempferol, fisetin, myricetin, and quercetin, have been found to be dual inhibitor targeting both PM II and FP-2. Fisetin and myricetin markedly inhibited PM II with IC_{50} = 7.8 and 7.2 μM, respectively and inhibited FP-2 with IC_{50} = 4.9 and 1.5 μM, respectively [17].

In our previous study, a series of chromone compounds were evaluated for their antimalarial activity against *P. falciparum* (structures and antimalarial activity as shown in Table 1) [18,19]. As a preliminary study to evaluate the potential of chromone series as dual inhibitor targeting PM II and FP-2, the docking simulation study of chromone compounds was performed in this study.

2. MATERIALS AND METHODS

The molecular docking study was performed using AutoDock version 4.2 (The Scripps Research Institute, Molecular Graphics Laboratory, USA) [20]. The study was carried out using the Lamarckian genetic algorithm, applying standard protocols of docking parameters as shown in Table 2. One hundred independent docking runs were used for each ligand. Results differing by less than 2.0 Å in positional root mean-square deviation (RMSD) were clustered together and represented by the result with the most favorable free energy of binding. The binding mode and binding free energy resulting from the docking were analyzed to evaluate the interaction between the ligand and the amino acid residues within the binding sites of PM II and FP-2.

Table 1. The antimalarial activity of chromone derivatives tested at the concentration 10 μg/mL.

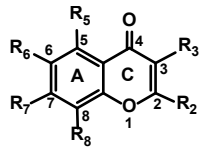

Compd	R_2	R_3	R_5	R_6	R_7	R_8	Antimalarial activity	
							% Inhibition	IC_{50} (μM)
1	Phenyl	H	H	H	H	OH	-3.82	-
3	Benzyl	H	H	H	OH	OH	96.90	9.43
4	Phenyl	H	H	H	OH	OH	71.90	19.66
5	CH3	H	H	H	OH	H	-0.69	-
11	3'-(CF3)-Phenyl	H	H	H	OH	H	56.80	14.69 ± 0.90
12	4'-(F)-Phenyl	H	H	H	OH	H	17.49	-
13	3',5'-(diNO2)-Phenyl	H	H	H	OH	H	95.62	10.30 ± 0.30
14	3'-(Cl)-Phenyl	H	H	H	OH	H	23.18	-
15	3',4'-(diCl)-Phenyl	H	H	H	OH	H	6.51	-
16	4'-(t-butyl)-Phenyl	H	H	H	OH	H	82.30	11.41
17	3'-(CF3)-Phenyl	H	OH	H	OH	H	84.10	11.07
18	4'-(F)-Phenyl	H	OH	H	OH	H	37.50	-
19	3',4'-(diF)-Phenyl	H	OH	H	OH	H	24.30	-
20	4'-(t-butyl)-Phenyl	H	OH	H	OH	H	95.20	9.15
22	3',5'-(diNO2)-Phenyl	H	OH	H	OH	H	-2.81	-
23	3'-(Cl)-Phenyl	H	OH	H	OH	H	76.20	13.83
24	3',4'-(diCl)-Phenyl	H	OH	H	OH	H	99.50	11.25
25	4'-(OCH3)-Phenyl	H	OH	H	OH	H	27.50	-
26	3'-(OCH3)-Phenyl	H	OH	H	OH	H	28.00	-
27	3'-(OCH3)-Phenyl	H	H	OH	H	H	68.00	13.23
28	3'-(Cl)-Phenyl	H	H	OH	H	H	39.52	-
29	4'-(F)-Phenyl	H	H	OH	H	H	49.12	-
31	4'-(t-butyl)-Phenyl	H	H	OH	H	H	8.40	-
32	3'-(CF3)-Phenyl	3"-(CF3)-benzoyl	H	H	OH	OH	8.40	-
33	3'-(Cl)-Phenyl	3"-(Cl)-benzoyl	H	H	OH	OH	24.20	-
34	3'-(OCH3)-Phenyl	3"-(OCH3)-benzoyl	H	H	OH	OH	98.38	3.82 ± 0.66
35	4'-(F)-Phenyl	4"-(F)-benzoyl	H	H	OH	OH	7.50	-
36	4'-(NO2)-Phenyl	4"-(NO2)-benzoyl	H	H	OH	OH	77.50*	0.95
37	4'-(OCH3)-Phenyl	4"-(OCH3)-benzoyl	H	H	OH	OH	66.19	9.32 ± 1.17
38	3',4'-(diF)-Phenyl	3",4"-(diF)-benzoyl	H	H	OH	H	65.10	12.40
39	3'-(CF3)-Phenyl	3"-(CF3)-benzoyl	H	H	OH	H	98.70	4.87
40	3'-(Cl)-Phenyl	3"-(Cl)-benzoyl	H	H	OH	H	23.40	-
41	3'-(OCH3)-Phenyl	3"-(OCH3)-benzoyl	H	H	OH	H	-1.50	-
42	4'-(F)-Phenyl	4"-(F)-benzoyl	H	H	OH	H	-0.08	-
43	4'-(NO2)-Phenyl	4"-(NO2)-benzoyl	H	H	OH	H	71.30	9.85
44	4'-(OCH3)-Phenyl	4"-(OCH3)-benzoyl	H	H	OH	H	93.17	11.73 ± 0.11
45	4'-(t-butyl)-Phenyl	4"-(t-butyl)-benzoyl	H	H	OH	H	98.50	5.46
46	3'-(OCH3)-Phenyl	3"-(OCH3)-benzoyl	OH	H	OH	H	65.93	10.47 ± 1.14
47	4'-(NO2)-Phenyl	4"-(NO2)-benzoyl	OH	H	OH	H	99.50	5.91
48	4'-(t-butyl)-Phenyl	4"-(t-butyl)-benzoyl	H	OH	H	H	89.07	9.33 ± 0.77
49	3'-(OCH3)-Phenyl	H	H	OH	OH	H	84.70	13.94
50	3'-(OCH3)-Phenyl	3"-(OCH3)-benzoyl	H	OH	OH	H	97.24	6.07 ± 0.41
		Chloroquine						0.42 ± 0.10 [18]
		Dihydroartemisinin						2.22 x 10-3 ± 0.24
		Mefloquine						5.71 x 10^{-2} ± 8.14

* activity tested at 1 μg/mL

Table 2. Docking and AutoGrid parameters used in docking simulation study.

	Parameters	
	PM II	**FP-2**
Docking parameters		
Number of GA run	100	100
Population size	150	150
Maximum number of energy evaluations	2,500,000	2,500,000
Maximum number of generation	27,000	27,000
Maximum number of top individuals that automatically survive	1	1
Rate of gene mutation	0.02	0.02
Rate of crossover	0.8	0.8
Mean of Cauchy distribution for gene mutation	0.0	0.0
Variance of Cauchy distribution for gene mutation	1.0	1.0
Number of generation for picking worst individual	10	10
Autogrid parameters		
PDB code	1SME	3BPF
Resolution (Å)	2.7	2.9
Num. Grid point in x, y, z	40, 54, 40	40, 30, 30
Spacing (Å)	0.375	0.375
Grid center	center on ligand	center on ligand
Smooth	0.5	0.5

Ligand preparation: The molecular structures of chromone compounds were sketched using SYBYL x2.0 (Tripos Associates, Saint Louis, MO, USA). Geometry optimization was performed using Powell method with a root-mean-squared energy gradient of 0.05 kcal/mol·Å. Tripos force field with Gasteiger-Hückel charges was employed during the energy minimization.

Receptor preparation: The crystal structures of PM II (PDB code 1SME) and FP-2 (PDB code 2BPF) complexed with the inhibitors (pepstatin A and N-[N-[1-hydroxycarboxyethyl-carbonyl] leucylamino-butyl]-guanidine, respectively) were retrieved from the Brookhaven Protein Data Bank (http://www.rcsb.org/pdb). The protein templates were prepared for docking study by removing all the native ligand structures and all water molecules from the complex structures. The polar hydrogen atoms were added and Gasteiger charges were assigned to protein atoms.

Docking method validation: The target enzyme templates were validated by re-docking which each ligand was docked back into the native protein. The re-docking was performed to verify that the docking method was reasonable and able to reproduce the orientation and position of the ligand observed in the crystal structure. The RMSD values of PM II and FP-2 were 0.43 Å and 1.28 Å, respectively.

Grid setup: The grid maps representing the protein in the actual docking process were calculated with AutoGrid. The grids were chosen to be sufficiently large to include the active site and significant portions of the surrounding surface. The parameters used in AutoGrid are shown in Table 2.

3. Results and Discussion

A series of forty-two chromone compounds were evaluated for antimalarial activity, the % inhibition and IC_{50} values as shown in Table 1 [18,19]. In this study, further investigation of the potential of chromone compounds as dual inhibitor targeting PM II and FP-2 was performed

using AutoDock program. Compounds which exhibited moderately to highly potent antimalarial activity (higher than 50% inhibition, IC_{50} = 0.95-19.66 μM) were chosen for the study. The crystal structures of PM II (PDB code 1SME) and FP-2 (PDB code 3BPF) were used to assess the binding interaction of chromone compounds against both enzymes templates. Conformations of the ligands were allowed to be flexible while the macromolecule target was fixed. The docking parameters and setting were given in materials and methods section.

The docking results were reported as binding energy (i.e., the lower the binding energy the higher the binding affinity). Table 3 shows the binding energies of the studied compounds together with their corresponding IC_{50} values. The binding energies of compounds against PM II were in the range of -5.93 to -9.03 kcal/mol and -4.75 to -8.00 kcal/mol for FP-2, indicating the good binding affinities to both PM II and FP-2. Compound **45** showed the strongest binding affinity to PM II (-9.03 kcal/mol) and also showed high binding affinity to FP-2 (-7.43 kcal/mol).

Table 3. The IC_{50} values and binding energies of chromone compounds from docking against PM II and FP-2.

Compd	IC_{50} (μM)	Binding energy (kcal/mole)	
	Antimalarial activity against *P. falciparum*	PM II	FP-2
3	9.43	-6.74	-6.20
4	19.66	-6.32	-6.22
11	14.69	-6.34	-4.97
13	10.30	-5.99	-5.92
16	11.41	-7.12	-6.18
17	11.07	-6.19	-4.75
20	9.15	-6.52	-4.87
23	13.83	-6.62	-5.03
24	11.25	-6.76	-5.28
27	13.23	-6.81	-5.87
34	3.82	-8.42	-7.28
36	0.95	-5.93	-6.07
37	9.32	-7.33	-6.63
38	12.40	-7.75	-6.51
39	4.87	-8.73	-6.26
43	9.85	-7.08	-7.76
44	11.73	-7.53	-6.60
45	5.46	-9.03	-7.43
46	10.47	-8.12	-7.03
47	5.91	-6.73	-8.00
48	9.33	-8.71	-7.33
49	13.94	-6.41	-5.46
50	6.07	-8.21	-6.52
Fisetin		-6.53	-4.97
Myricetin		-5.51	-4.78

Compound **47** was found to best dock with FP-2 (-8.00 kcal/mol) and good binding to PM II (-6.73 kcal/mol). Moreover, compounds **45** and **47** displayed stronger binding to both enzymes than the known dual PM II and FP-2 inhibitors, fisetin and myricetin. The binding energies of fisetin against PM II and FP-2 obtained from the same docking study were -6.53 and -4.97 kcal/mol, respectively while myricetin showed binding energies = -5.51 and -4.78 kcal/mol, respectively. Most of the compounds containing substituents at position 3 (i.e., $R_3 \neq H$) of the chromone nucleus showed the higher potency (IC_{50} = 0.95-12.40 μM, Table 3). These compounds also exhibited better binding energies with PM II (-5.93 to -9.03 kcal/mol) and FP-2 (-6.07 to -8.00 kcal/mol) when compared with the 3-unsubstitued compounds.

The binding interactions of compound **45** against PM II and FP-2 comparing with fisetin and myricetin are depicted in Figure 1. Figure 1a shows compound **45** binding with PM II in different orientation from fisetin and myricetin. The chromone nucleus of compound **45** positioned in S1´ (Ser37, Met75) and S2´ (Asn76, Tyr77, Val78, Tyr192) subsites. The phenyl ring was in S1 (Ile32, Ser79, Phe111, Gly216) and S3 (Met15, Thr114) subsite. The benzoyl ring lied in S2 (Thr217, Thr221, Ile290, Leu292, Ile300) and S4 (Ser218, Ala219, Asn288) subsites. The chromone nucleus of fisetin and myricetin occupied the S2 and S4 instead of S1´ and S2´ subsites as for compound **45**. Figure 1b illustrates the binding mode of compound **45** with FP-2. The chromone nucleus of compound **45** pointed toward S1 (Gln36, Cys39, Cys42, Asn173, His174) similar to those of fisetin and myricetin. The phenyl ring of compound **45** lied in S3 (Tyr 78, Gly83, Leu84) and the benzoyl ring in S2 (Trp43, Ile85, Ser149, Asp234). It was found that the hydroxy group at C-7 position (ring A) formed hydrogen bond with Asn76 in PM II, while the carbonyl oxygen at C-4 position (ring C) made hydrogen bond with His174 in FP-2.

The binding interactions of compound **47** against PM II and FP-2 are shown in Figure 2. Figure 2a shows the chromone nucleus of compound **47** positioned in the same subsites (S1´ and S2´) as compound **45** but flipping in opposite orientation. The phenyl ring was in S2 and S4 and the benzoyl ring in S1 and S3 subsites. The binding mode of compound **47** in the binding site of FP-2 (Figure 2b) was different from those of compound **45**. The chromone nucleus of compound **47** pointed toward S3 subsite. The phenyl ring of compound **47** lied in S2 and the benzoyl ring in S1. The chromone nucleus of fisetin and myricetin occupied S1 subsite. The docking results showed that the hydroxyl group at C-5 formed hydrogen bond with Gly36 in PM II and with Asn81 in FP-2. The schematic view of the binding modes of compounds **36**-**37**, **43**-**45** and **48** with PM II and compounds **36**, **43**, **46**-**47** and **50** with FP-2 binding sites are summarized in Figures 3a and 3b, respectively.

Compound **34** was another interesting compound (IC_{50} = 3.82 μM) showing high binding energy with both PM II and FP-2 (binding energies = -8.42 and -7.28 kcal/mol, respectively). In the PM II binding site (Figure 4a), the chromone nucleus of compound **34** lied in the same subsites (S2 and S4) as fisetin and myricetin. The phenyl ring was in S1 and S3 and the benzoyl ring in S1´ and S2´ subsites while the phenyl ring of fisetin and myricetin positioned in S1, S1´ and S2´ subsites. In FP-2 binding site (Figure 4b) the chromone nucleus of compound **34** was located in the same subsite (S3) as compound **47** but pointing toward opposite direction. The phenyl ring positioned in S1 and the benzoyl ring in S2 subsite. The chromone nucleus of fisetin and myricetin were in S1 subsite instead of S3 as described for compound **34**. The hydroxyl group at C-7 formed hydrogen bond with Ser218 in PM II while the hydroxyl at C-8 formed hydrogen bond with Asn81 in FP-2.

The binding modes of chromone compounds with PM II and FP-2 are summarized in Tables 4 and 5, respectively. In general, as shown in Tables 4 and 5, chromone compounds displayed the similar binding orientation to fisetin and myricetin against

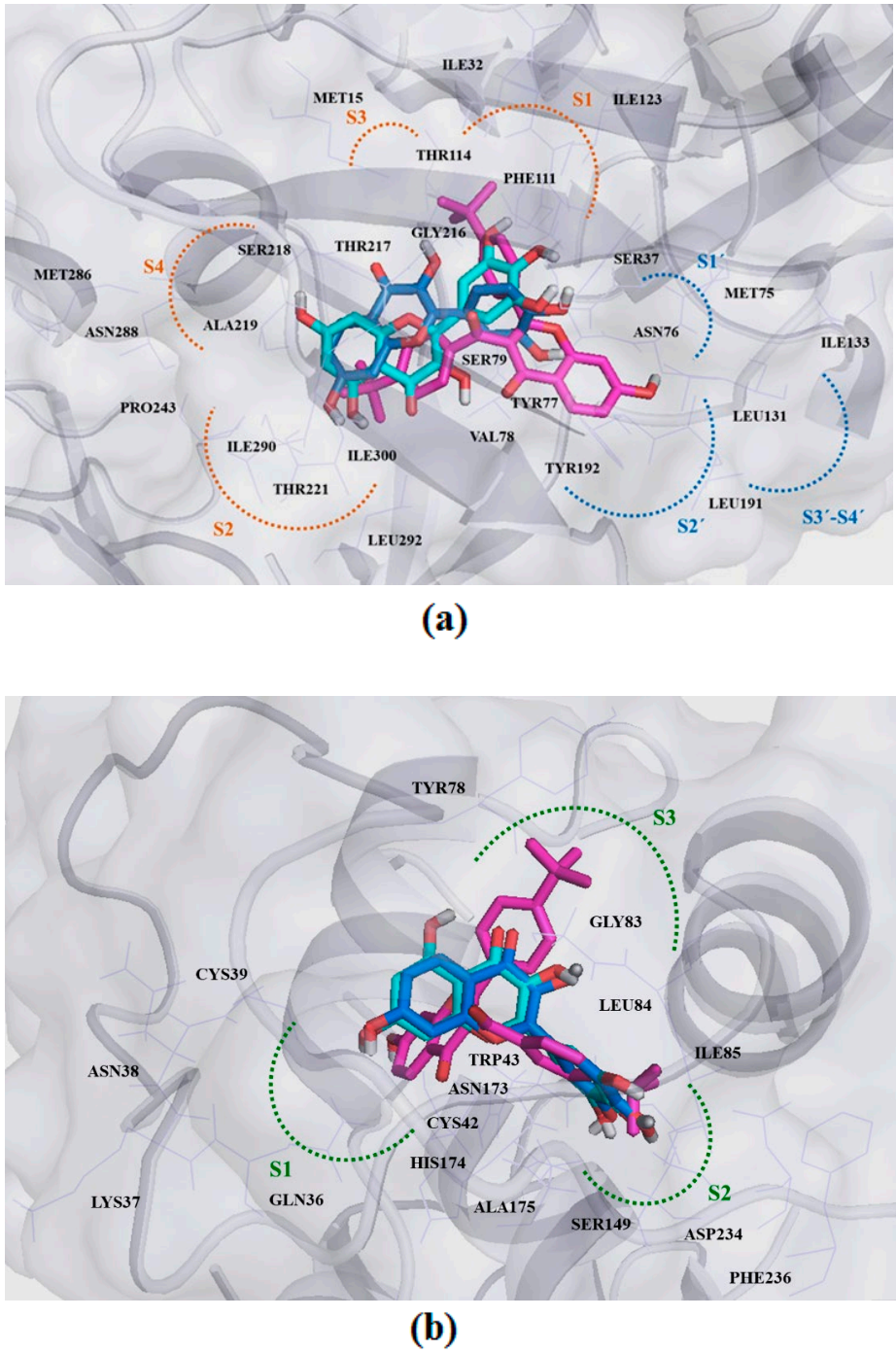

Figure 1. The binding interaction of compound **45** (purple) to amino acid residues in (a) PM II and (b) FP-2 binding sites, comparing with fisetin (blue) and myricetin (cyan).

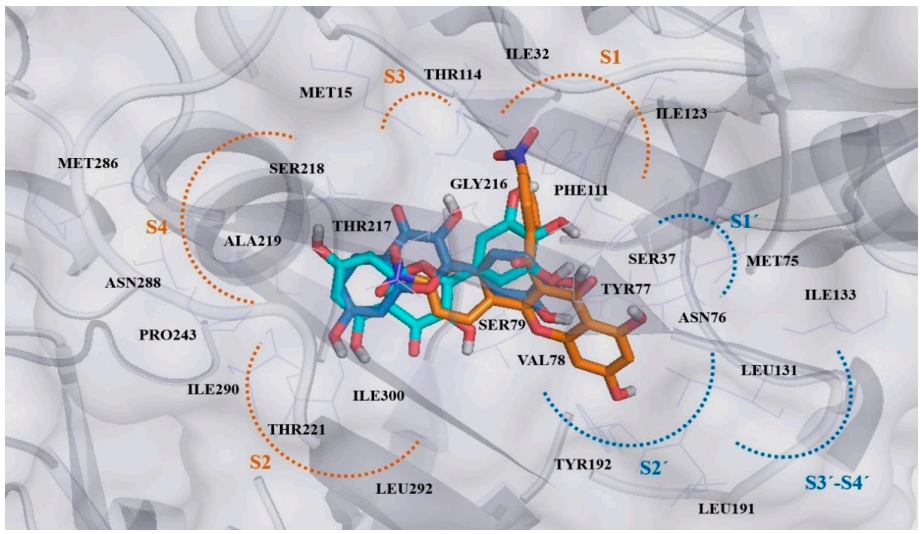

(a)

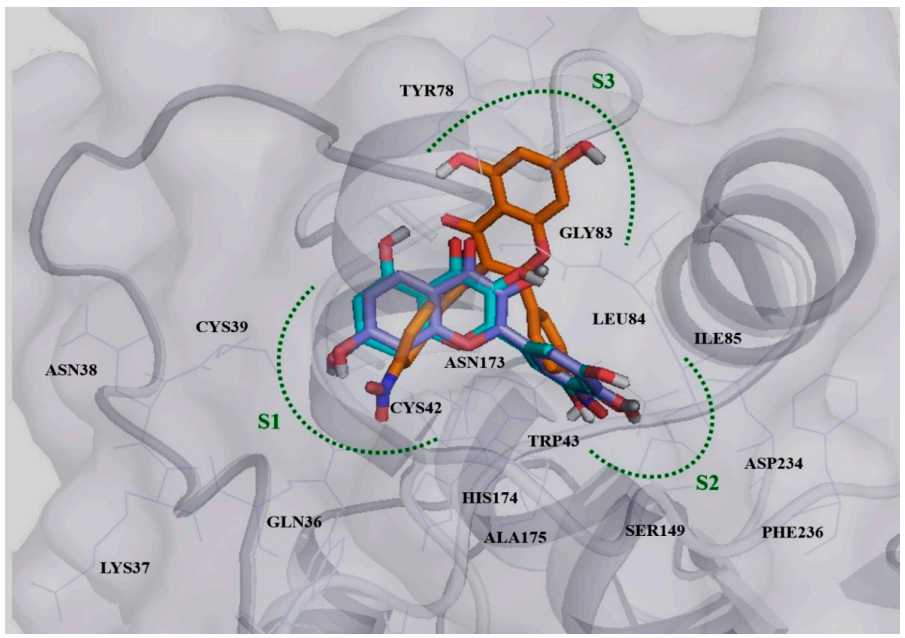

(b)

Figure 2. The binding interaction of compound **47** (orange) to amino acid residues in (a) PM II and (b) FP-2 binding sites, comparing with fisetin (blue) and myricetin (cyan).

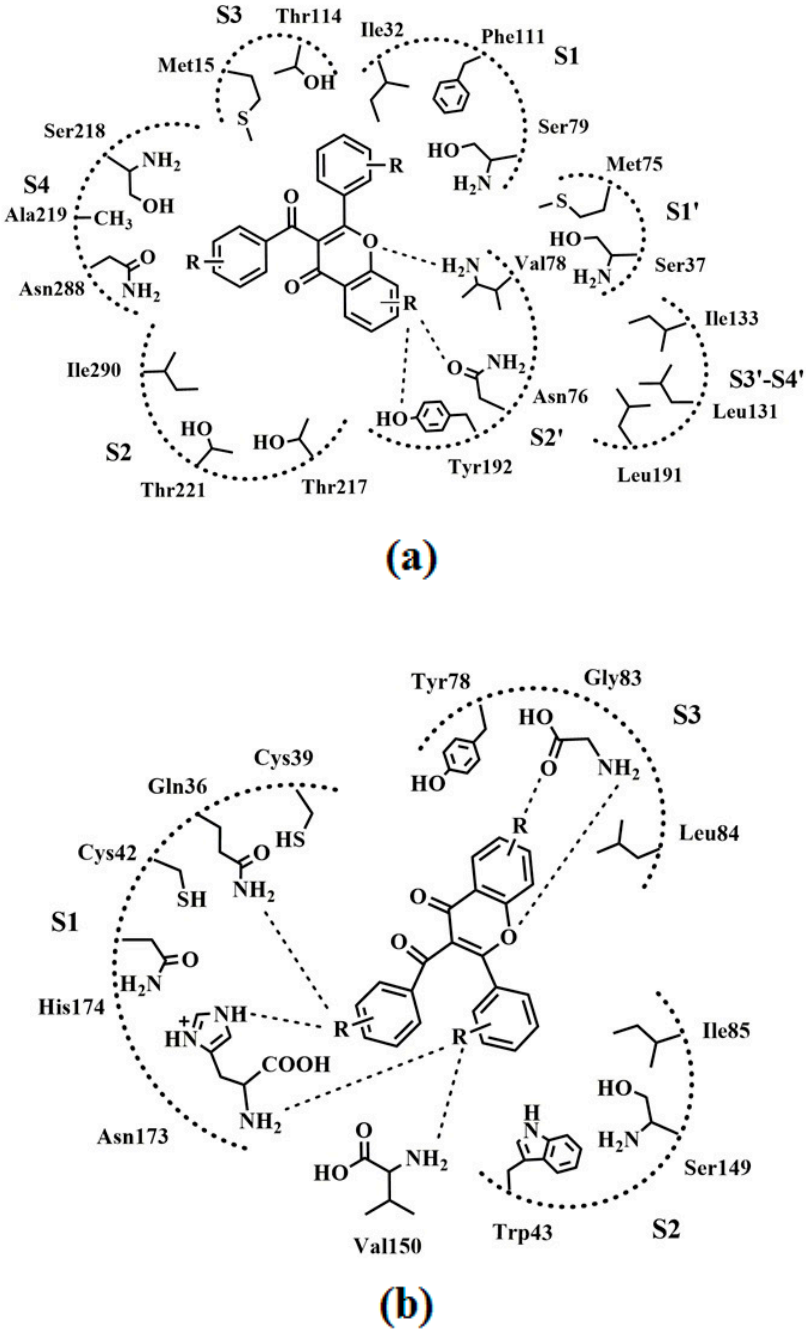

Figure 3. The schematic view of the binding modes showing the interacted amino acid residues and H-bond (dotted line) (a) compounds **36**-**37**, **43**-**45** and **48** in PM II binding sites and (b) compounds **36**, **43**, **46**-**47** and **50** in FP-2 binding sites.

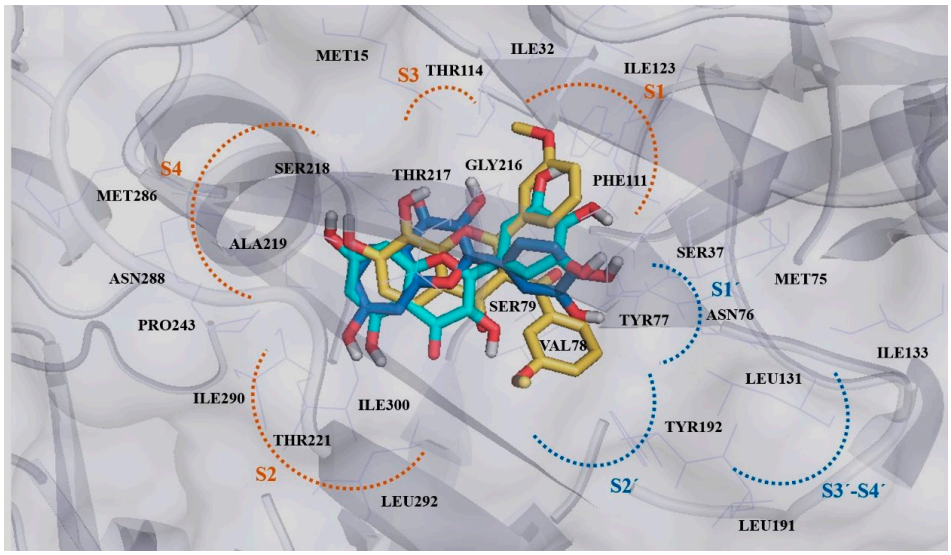

(a)

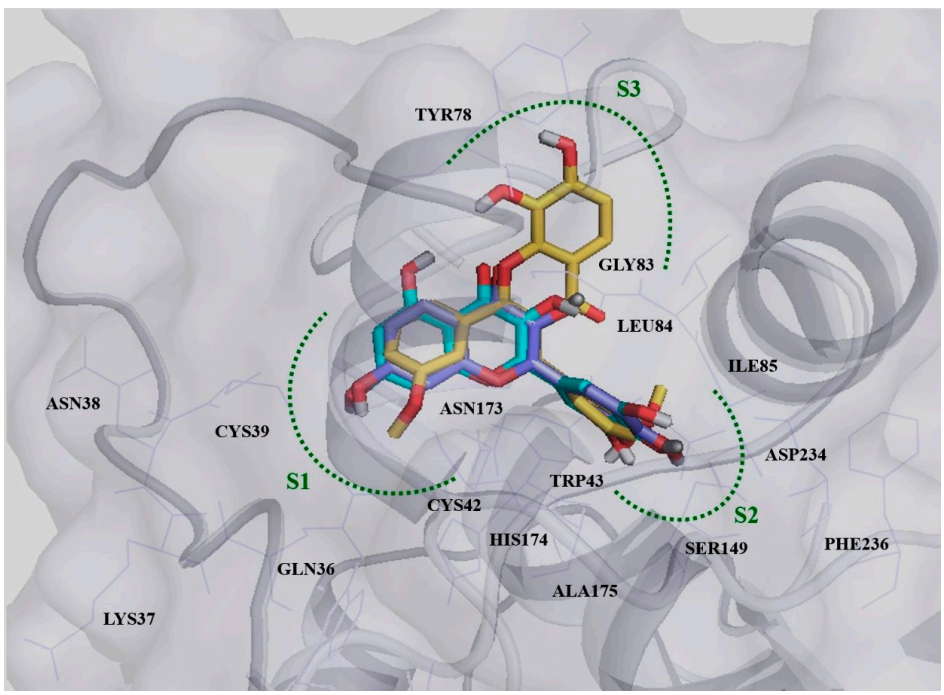

(b)

Figure 4. The binding interaction of compound **34** (yellow) to amino acid residues in (a) PM II and (b) FP-2 binding sites, comparing with fisetin (blue) and myricetin (cyan).

PM II. In contrast, the binding orientation of chromone compounds in FP-2 binding site was remarkably different from fisetin and myricetin. As to PM II, the docking results illustrated that the C-7 hydroxyl group played an important role in forming hydrogen bond interaction with the enzyme. The highly potent compounds (i.e., **16**, **34**, **37**-**39**, **43**-**46**, and **50**) contained this key hydroxyl moiety and these compounds showed good binding energy (-7.08 to -9.03 kcal/mol). In the case of FP-2, there were no apparent structural features that could explain the better binding energy of the compounds **34**, **43**, **45**, **47** and **48**. However, as mentioned above, compounds with substituents at position 3 tended to have tight binding with FP-2.

Table 4. The binding modes of fisetin, myricetin and chromone compounds in PM II binding site.

Compd	Structure	Binding mode	H-bond interacted residues (distance Å)
Fisetin	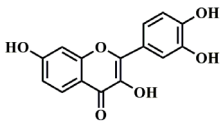	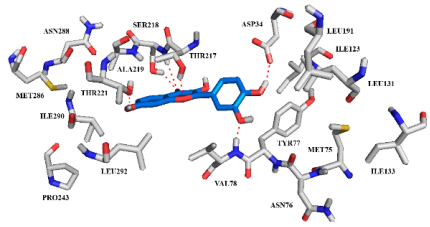	Thr221 (1.890) Ser218 (2.153) Ser218 (2.742) Thr217 (1.915) Asp34 (2.004) Val78 (1.736)
Myricetin	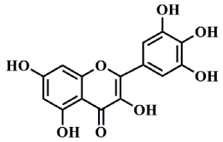	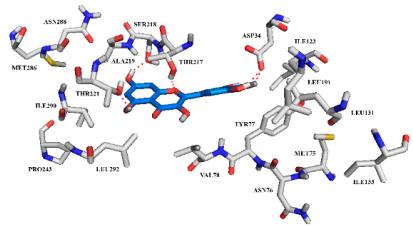	Thr221 (1.951) Ser218 (1.888) Thr217 (2.332) Asp34 (1.905) Asp34 (1.692)
34	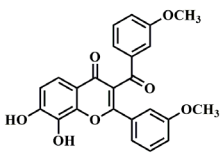	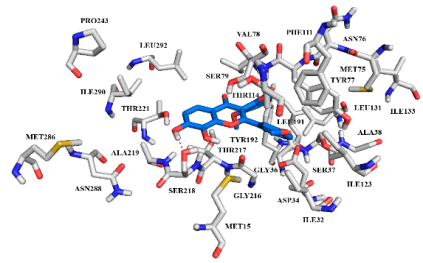	Ser218 (1.811)

Table 4. The binding modes of fisetin, myricetin and chromone compounds in PM II binding site. (Continued)

Compd	Structure	Binding mode	H-bond interacted residues (distance Å)
38	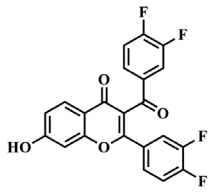	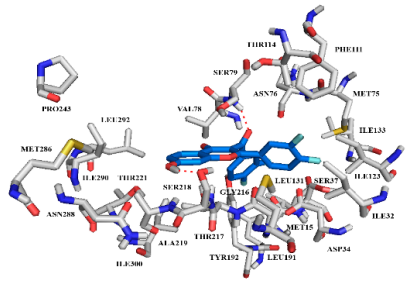	Ser218 (1.890) Ser79 (1.989)
43	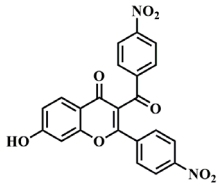	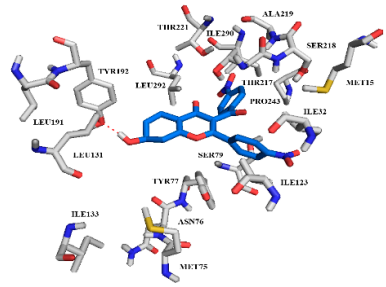	Tyr192 (1.930)
45	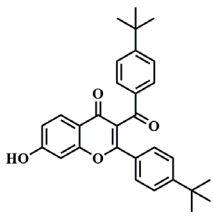	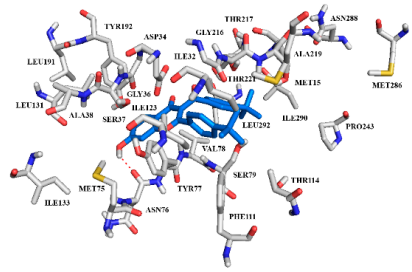	Asn76 (2.105)
47	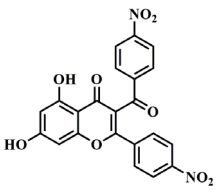	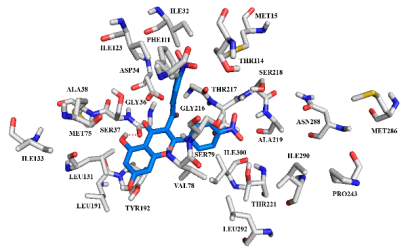	Gly36 (2.254)

Table 4. The binding modes of fisetin, myricetin and chromone compounds in PM II binding site. (Continued)

Compd	Structure	Binding mode	H-bond interacted residues (distance Å)
48	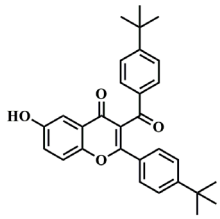	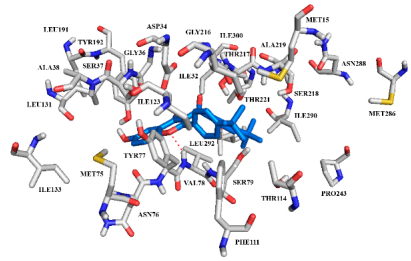	Val78 (2.535)
50	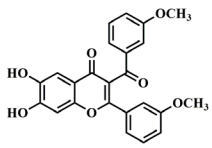	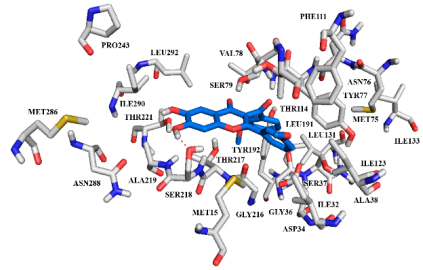	Ser218 (1.869)

Table 5. The binding modes of fisetin, myricetin and chromone compounds in FP-2 binding site.

Compd	Structure	Binding mode	H-bond interacted residues (distance Å)
Fisetin	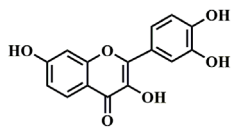	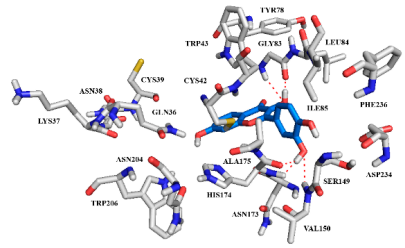	Gly83 (2.691) Gly83 (1.689) Val150 (2.916) His174 (2.590) His174 (1.984)
Myricetin	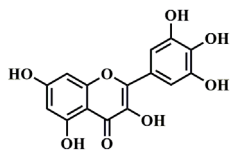	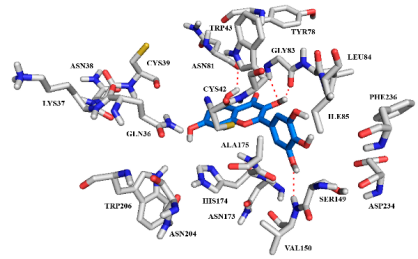	Asn81 (2.171) Gly83 (2.338) Gly83 (1.837) Val150 (2.954)

Table 5. The binding modes of fisetin, myricetin and chromone compounds in FP-2 binding site.

Compd	Structure	Binding mode	H-bond interacted residues (distance Å)
34	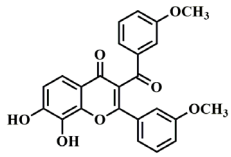	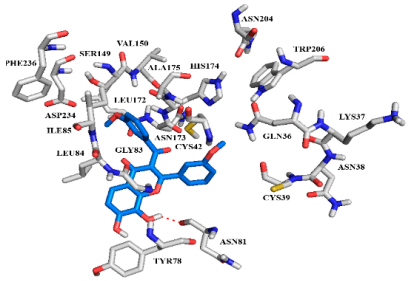	Asn81 (1.987)
38	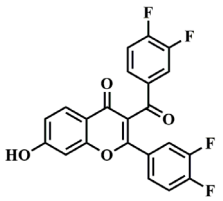	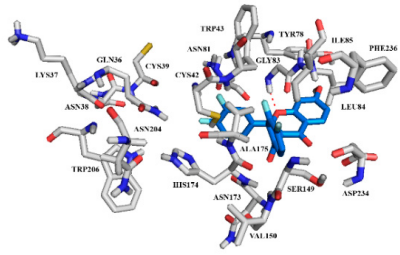	Gly83 (1.922)
43	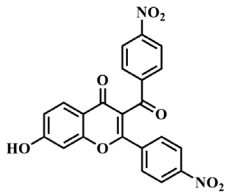	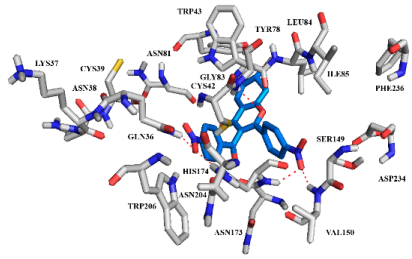	Val150 (2.216) His174 (2.168) His174 (2.099) Gln36 (2.346) Gly83 (2.805)
45	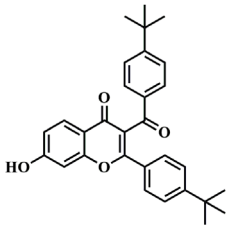	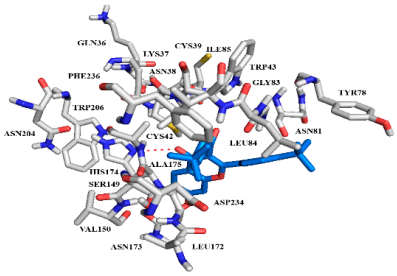	His174 (2.312)
47	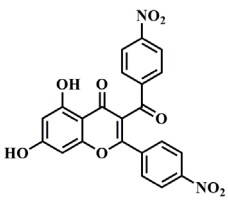	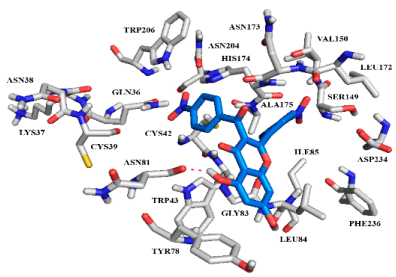	Asn81 (1.823)

Table 5. The binding modes of fisetin, myricetin and chromone compounds in FP-2 binding site. (Continued)

Compd	Structure	Binding mode	H-bond interacted residues (distance Å)
48	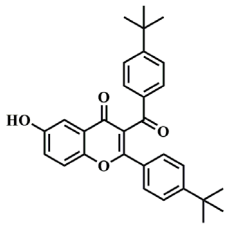	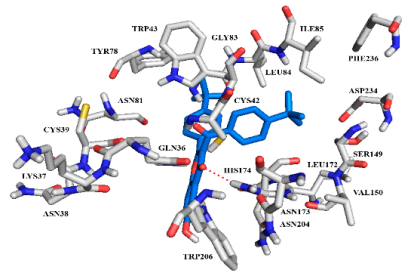	His174 (3.007)
50	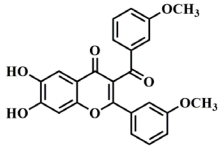	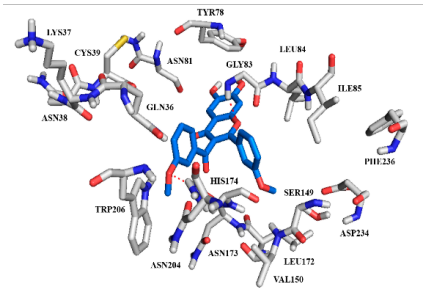	His174 (2.000) Gly83 (2.248)

4. Conclusions

From the docking results, chromone compounds showed high binding affinities to both PM II and FP-2 and even higher than those of fisetin and myricetin. Preliminary structure-activity relationship could be deduced from the results that the compounds containing substituents at position 3 of the chromone nucleus were found to exhibit better binding affinity against both PM II and FP-2. In case of PM II, the C-7 hydroxyl group played a key role in forming hydrogen bond interaction with PM II. This dual inhibitory activity against both enzymes might as well accounted for their antimalarial activity. Though the mechanism underlying the antimalarial activity still needs further investigation, the results from this study lead to the potential of chromone compounds as new antimalarial agent with dual inhibitory activity against PM II and FP-2.

Acknowledgement

The authors thank the High Performance Computer Center (HPCC), National Electronic and Computer Technology Center (NECTEC) of Thailand for providing SYBYL facilities.

References

[1] Cui L., Mharakurwa S., Ndiaye D., Rathod P.K. and Rosenthal P.J., *Am. J. Trop. Med. Hyg.*, 2015; **93(3 Suppl)**: 57-68. DOI 10.4269/ajtmh.15-0007.

[2] Ashley E.A., Pyae Phyo A. and Woodrow C.J., *Lancet*, 2018; **391**: 1608-1621. DOI 10.1016/S0140-6736(18)30324-6.

[3] Coombs G.H., Goldberg D.E., Klemba M., Berry C., Kay J. and Mottram J.C., *Trends Parasitol.*, 2001; **17(11)**: 532-537. DOI 10.1016/s1471-4922(01)02037-2.

[4] Banerjee R., Liu J., Beatty W., Pelosof L., Klemba M. and Goldberg D.E., *Proc. Natl. Acad. Sci. U.S.A.*, 2002; **99**: 990-995. DOI 10.1073/pnas.022630099.

[5] Song Y., Jin H., Liu X., Zhu L., Huang J. and Li H., *Bioorg. Med. Chem. Lett.*, 2013; **23(7)**: 2078-2082. DOI 10.1016/j.bmcl.2013.01.128.

[6] Silva A.M., Lee A.Y., Gulnik S.V., Maier P., Collins J., Bhat T.N., Collins P.J., Cachau R.E., Luker K.E., Gluzman I.Y., Francis S.E., Oksman A., Goldberg D.E. and Erickson J.W., *Proc. Natl. Acad. Sci. U.S.A.*, 1996; **93(19)**: 10034-10039. DOI 10.1073/pnas.93.19.10034.

[7] Shenai B.R., Sijwali P.S., Singh A. and Rosenthal P.J., *J. Biol. Chem.*, 2000; **275**: 29000-29010. DOI 10.1002/med.20163.

[8] Subramanian S., Sijwali P.S. and Rosenthal P.J., *J. Biol. Chem.*, 2007; **282(34)**: 24961-24969. DOI 10.1074/jbc.M703316200.

[9] Kerr I.D., Lee J.H., Pandey K.C., Harrison A., Sajid M., Rosenthal P.J. and Brinen L.S., *J. Med. Chem.*, 2009; **52(3)**: 852-857. DOI 10.1021/jm8013663.

[10] Ehmke V., Kilchmann F., Heindl C., Cui K., Huang J., Schirmeister T. and Diederich F., *Med. Chem. Commun.*, 2011; **2**: 800-804. DOI 10.1039/C1MD00115A.

[11] Munkhjargal T., AbouLaila M., Terkawi M.A., Sivakumar T., Ichikawa M., Davaasuren B., Nyamjargal T., Yokoyama N. and Igarashi I., *Am. J. Trop. Med. Hyg.*, 2012; **87(4)**: 681-688. DOI 10.4269/ajtmh.2012.12-0218.

[12] Bhaumik P., Gustchina A. and Wlodawer A., *Biochim. Biophys. Acta*, 2012; **1824(1)**: 207-223. DOI 10.1016/j.bbapap.2011.04.008.

[13] Micale N., Kozikowski A.P., Ettari R., Grasso S., Zappala M., Jeong J.J., Kumar A., Hanspal M. and Chishti A.H., *J. Med. Chem.*, 2006; **49(11)**: 3064-3067. DOI 10.1021/jm060405f.

[14] Verissimo E., Berry N., Gibbons P., Cristiano M.L.S., Rosenthal P.J., Gut J., Ward S.A. and O'Neill P.M., *Bioorg. Med. Chem. Lett.*, 2008; **18(14)**: 4210-4214. DOI 10.1016/j.bmcl.2008.05.068.

[15] Tasdemir D., Gabriela L., Brun R., Rüedi P., Scapozza L. and Perozzo R., *J. Med. Chem.*, 2006; **49**: 3345-3353. DOI 10.1021/jm0600545

[16] Lehane A.M. and Saliba K.J., *BMC Res. Notes*, 2008; **1**: 26-31. DOI 10.1186/1756-0500-1-26.

[17] Jin H., Xu Z., Cui K., Zhang T., Lu W. and Huang J., *Fitoterapia*, 2014; **94**: 55-61. DOI 10.1016/j.fitote.2014.01.017.

[18] Lerdsirisuk P., Maicheen C. and Ungwitayatorn J., *Bioorg. Chem.*, 2014; **57**: 142-147. DOI 10.1016/j.bioorg.2014.10.006.

[19] Maicheen C., *Cyclooxygenase-2 Inhibitory Activity and Antimalarial Activity of Chromone Derivatives,* PhD Thesis, Mahidol University, Thailand, 2018.

[20] Morris G.M., Huey R., Lindstrom W., Sanner M.F., Belew R.K., Goodsell D.S. and Olson, A.J., *J. Comput. Chem.*, 2009; **30(16)**: 2785-2791. DOI 10.1002/jcc.21256.